CHAPTER 8

THERMAL ANALYSIS AND AGEING CHARACTERISTICS OF NBR/EVA BLENDS

The results of this chapter have been accepted for publication in *J. Thermal Analysis*

Thermal degradation of polymers is an important subject as it covers a broad field, ranging from the development of thermoresistant polymers and ablation problems to the stabilisation of thermolabile polymers. Thermogravimetric analysis (TGA) has proved itself as a successful technique in determining the thermal stability of polymers and polymer blends. A knowledge of degradation and decomposition changes in polymers on heating is important when these materials are processed and fabricated for use. The threshold temperature for breakdown determines the upper limit of temperature in fabrication.[1,2] In differential scanning calorimetry (DSC), the heat flow rate associated with a thermal event can be measured as a function of time and temperature allowing us to obtain quantitative information about melting and phase transitions of the blend. Under different environmental conditions most polymers and their products gradually lose their useful properties as a result of polymer chain degradation. Heat is one of the degrading agents and its effect can be studied by thermal ageing.

The thermal stability of individual polymers is greatly influenced by blending. It depends strongly on the interactions of the component polymers. The thermal stability of poly(vinyl chloride)/epoxidised natural rubber (PVC/ENR) blends is greatly influenced by the interaction between PVC and ENR, which is a miscible system.[3] Varughese *et al.*[4] studied the miscibility of PVC with 50% epoxidised natural rubber (ENR) using DSC. A single T_g between the T_gs of the

pure components revealed the miscibility of the system. A comparison of thermal behaviour of miscible and immiscible blends was reported from this laboratory by Lizymol and Thomas.[5] In the case of completely miscible PVC/EVA system, the thermal stability of PVC is considerably improved by the addition of EVA. But in the case of partially miscible PVC/styrene-acrylonitrile copolymer (SAN) and completely immiscible EVA/SAN blends, the decomposition behaviour of individual polymers are retained in the blend. The thermal properties of a ternary blend of PVC/EVA/SAN are also reported by them.[6] In this ternary system there is a thermodynamically miscible region in which PVC acts as an interfacial agent for the immiscible SAN/EVA system and the overall thermal stability of the ternary blend is superior to the homopolymers and PVC/SAN and SAN/EVA blends.

Thermogravimetric analysis of aromatic polyoxadiazole/polyamide-6 shows that the temperature of degradation of PA-6 in the blends decreases with the addition of more than 10 weight per cent of polyoxadiazole.[7] Amraee *et al.*[8] used thermogravimetric analysis for the quantitative and qualitative identification of SBR/BR blends. They also checked the uniformity of mixing and differentiated oil extended SBR from non extended SBR. Sequential interpenetrating polymer networks (IPN) based on nitrile rubber (NBR) and poly(vinyl acetate) (PVA) have been synthesised by Patri *et al.*[9] DSC measurements showed single T_g value for all the IPNs. Calorimetric analysis showed that poly(vinyl acetate) tends to compatibilise blends of PVF_2/PS.[10] The miscibility and melting behaviour of blends of vinylidene fluoride with tetrafluoroethylene and hexafluoroacetone copolymers were investigated calorimetrically by Cho *et al.*[11]

During thermal ageing main chain scission, crosslink formation and crosslink breakage can take place. It is also possible that the existing crosslinks may breakdown and a more stable crosslink can be formed. The extent of change in property is governed by the relative ratios and magnitudes of such reactions. Thomas and co-workers have reported the ageing of polymer blends and composites.[12-14] The addition of poly(vinyl chloride) to nitrile rubber yielded

advantages in thermal ageing, ultraviolet and ozone resistance.[15] Noland *et al.*[16] noted that the ultraviolet degradation of the poly(methyl methacrylate)/ poly(vinylidene fluoride) blends is consistent with that of the two components considered separately. Weatherable film applications of this blend are possible because of the high resistance of both the components to UV degradation. Blending of natural rubber and polybutadiene have shown various advantages including heat stability and abrasion resistance.[17] The photodegradation of ethylene vinyl acetate copolymer/poly(vinyl chloride) and nitrile rubber/poly(vinyl chloride) blends has been studied by Skowronski *et al.*[18] The thermo-oxidative ageing of rubbers is reported by several authors.[19,20]

This chapter deals with the thermal analysis and ageing of NBR/EVA blends. The effect of blend composition, crosslinking systems, and fillers on thermal degradation of the blends is studied. The influence of these parameters on thermal ageing of the blends is also investigated. The melting and phase transition temperatures are measured calorimetrically.

8.1 Results and discussion

8.1.1 Thermogravimetric analysis

(a) Effect of blend composition

The thermogravimetric plots of peroxide cured EVA and NBR are shown in Figures 8.1 and 8.2 respectively. Two regions of degradation of EVA are evident (Figure 8.1). The first step degradation starts at about 310°C and is completed at 427°C. The second stage degradation occurs in the region 446-538°C. The former stage of the degradation is due to the elimination of acetic acid from the vinyl acetate part of the chain and the later stage of degradation is due to scission of polyene left after deacetylation.[1]

$$(-CH_2-CH_2-CH_2-\underset{\displaystyle COOCH_3}{\underset{|}{CH}}-)_n \xrightarrow{320\text{-}330^\circ C} nCH_3-COOH + (-CH_2-CH_2-CH=CH-)_n$$

$$(-CH_2-CH_2-CH=CH-)_n \xrightarrow[\text{Scission}]{440\text{-}450^\circ C} \text{Hydrocarbons}$$

The weight loss observed during the first and second stages are 18.7 and 79.4% respectively. About 1.9% remains as residue above 538°C. The weight loss observed at 350°C is 4.81% and that at 475°C is 43.5%. In the DTG curve the major peak is observed at 493°C which corresponds to the scission of conjugated polyene left after deacetylation. A small peak corresponding to the deacetylation is observed at 387°C.

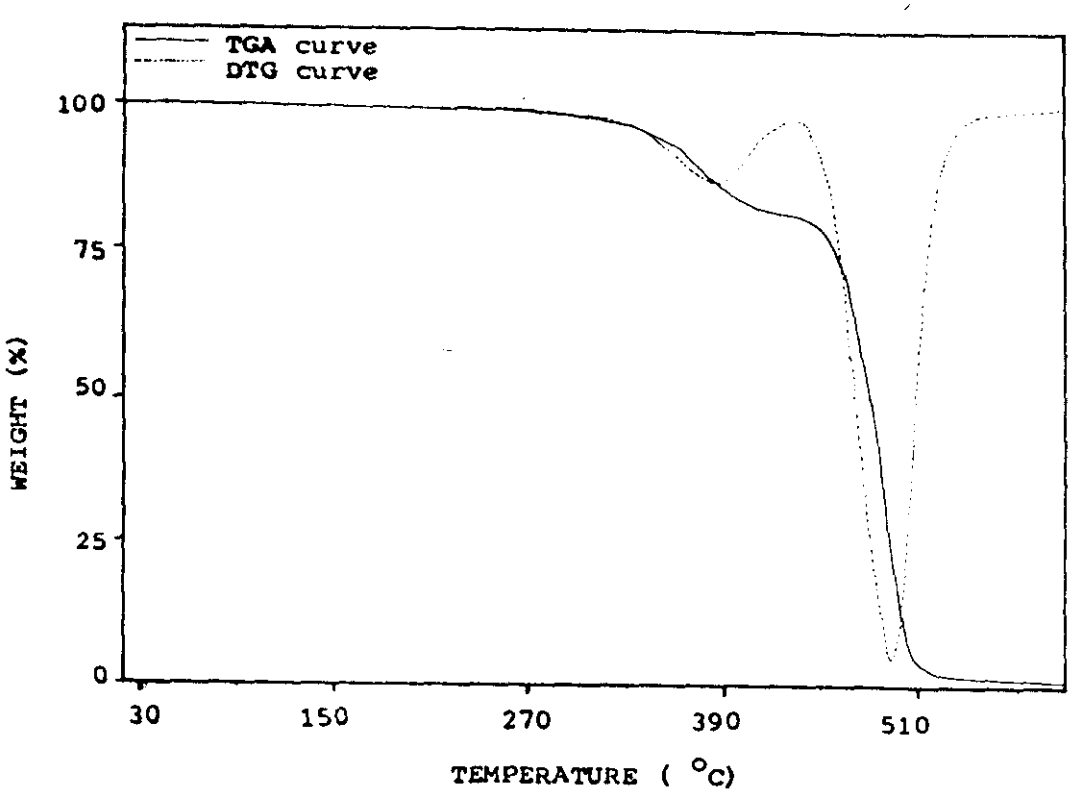

Figure 8.1. TG and DTG curves of peroxide cured EVA

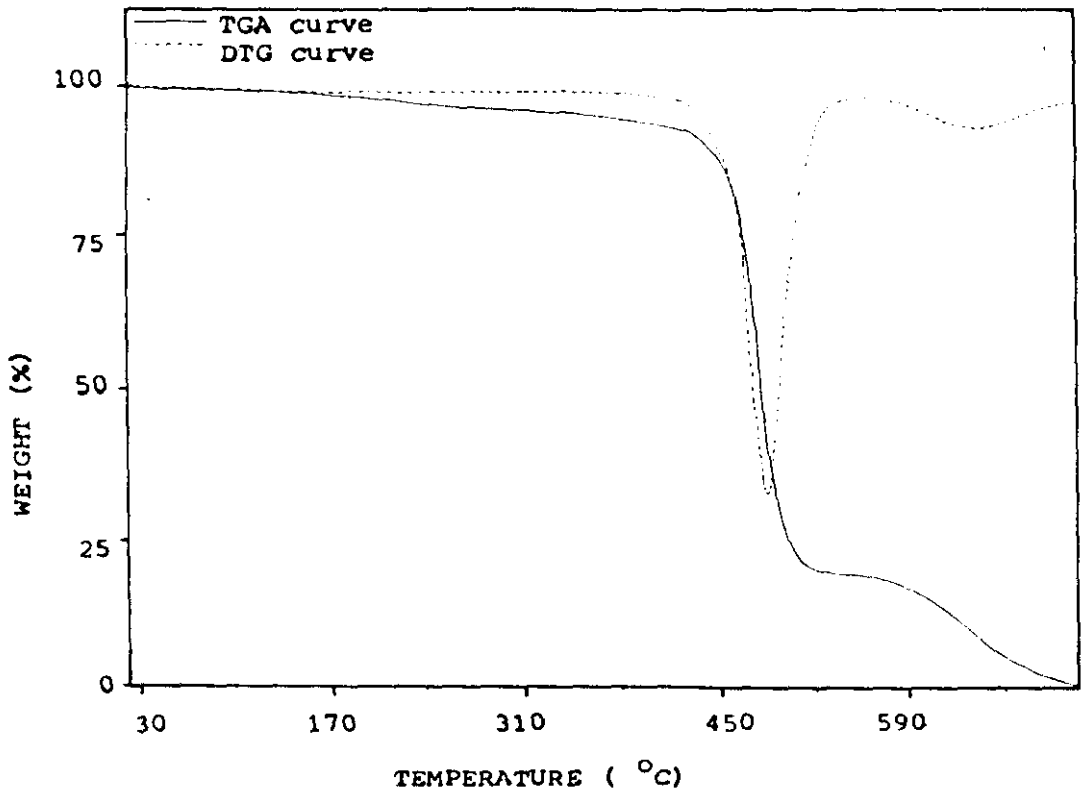

Figure 8.2. TG and DTG curves of peroxide cured NBR

In the case of nitrile rubber (NBR) also a two step degradation is observed. (Figure 8.2) Due to the presence of acrylonitrile and butadiene units in nitrile rubber, degradation occurs via a two stage mechanism.[7] The first step degradation is from 427–536°C and the second step from 584–706°C. A weight loss of 80.5 and 18% are observed during the first and second steps of degradation respectively. About 1.5% remains as residue above 692°C. The weight loss observed at 350°C is 4.8% and that at 475°C is 33.1%. In the DTG curve, a major peak at 488 and minor peak at 638°C are observed. The peak at 488°C is due to the degradation of butadiene segments which will be completed around 500°C[1] and the peak at 638°C corresponds to the degradation of acrylonitrile segments.

In general, the degradation behaviour of the blends is marginally different from that of the individual components. It has been reported that the thermal stability can be improved by the incorporation of a second polymer.[20] The TG and DTG curves of NBR/EVA blends i.e., 30/70 ($N_{30}P$), 50/50 ($N_{50}P$), 70/30 ($N_{70}P$) are given in Figures 8.3–8.5 respectively.

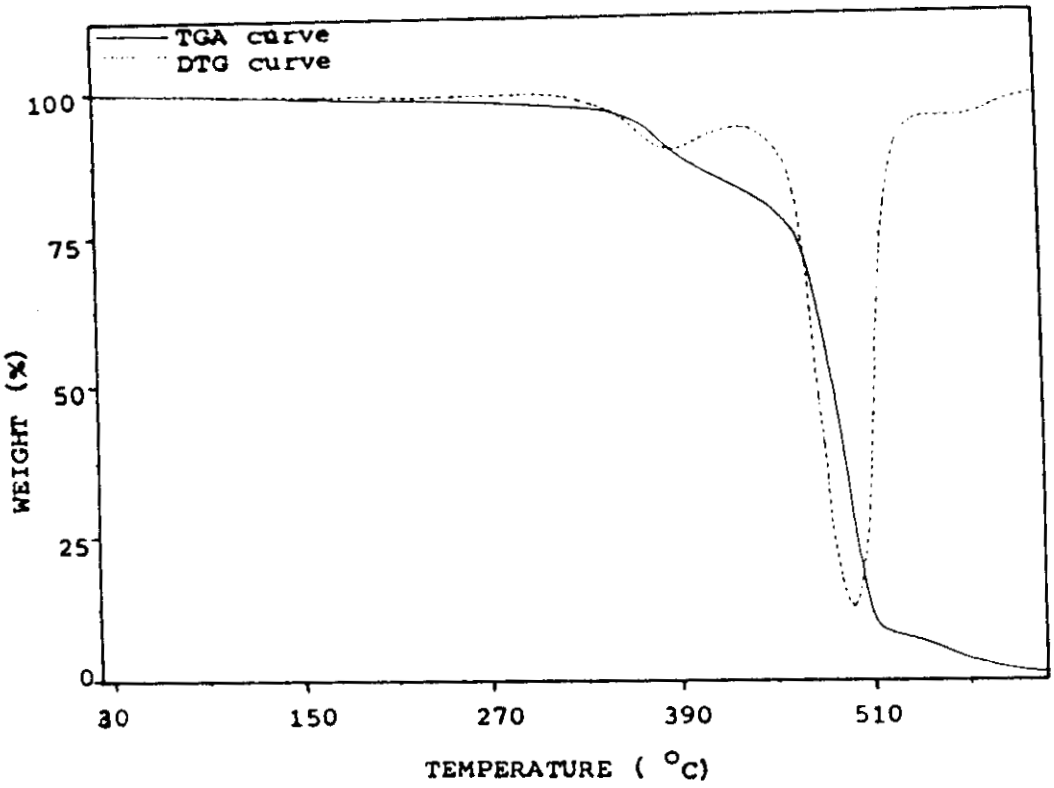

Figure 8.3. TG and DTG curves of $N_{30}P$

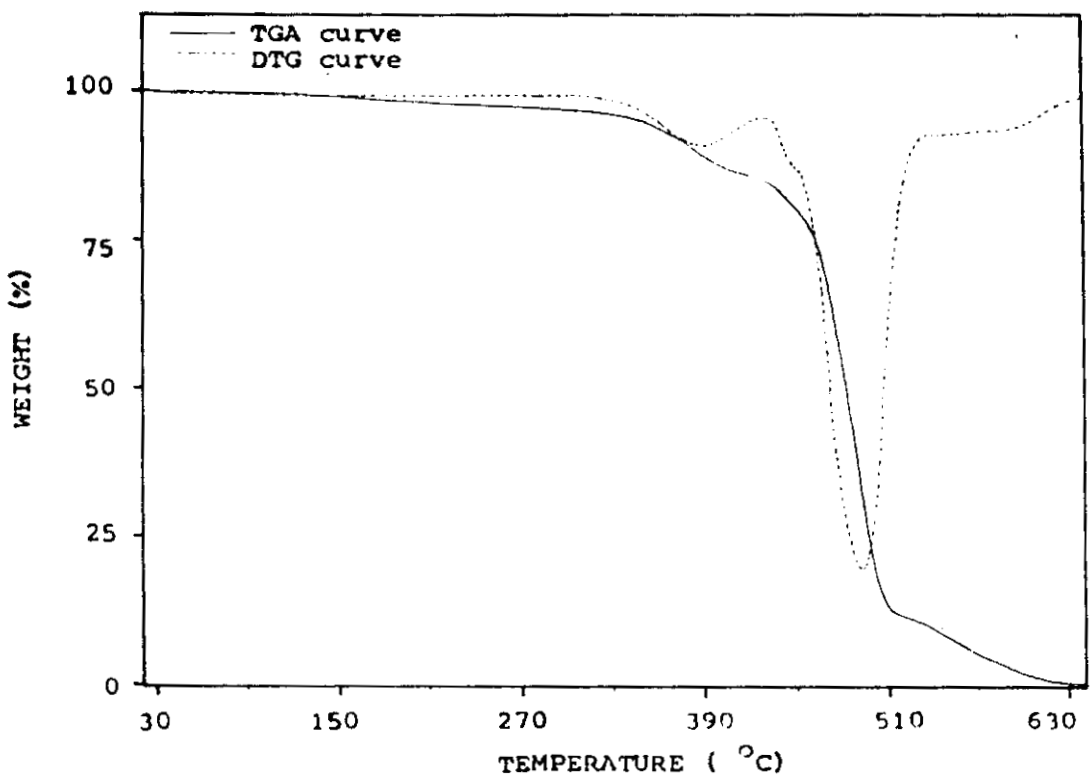

Figure 8.4. TG and DTG curves of $N_{50}P$

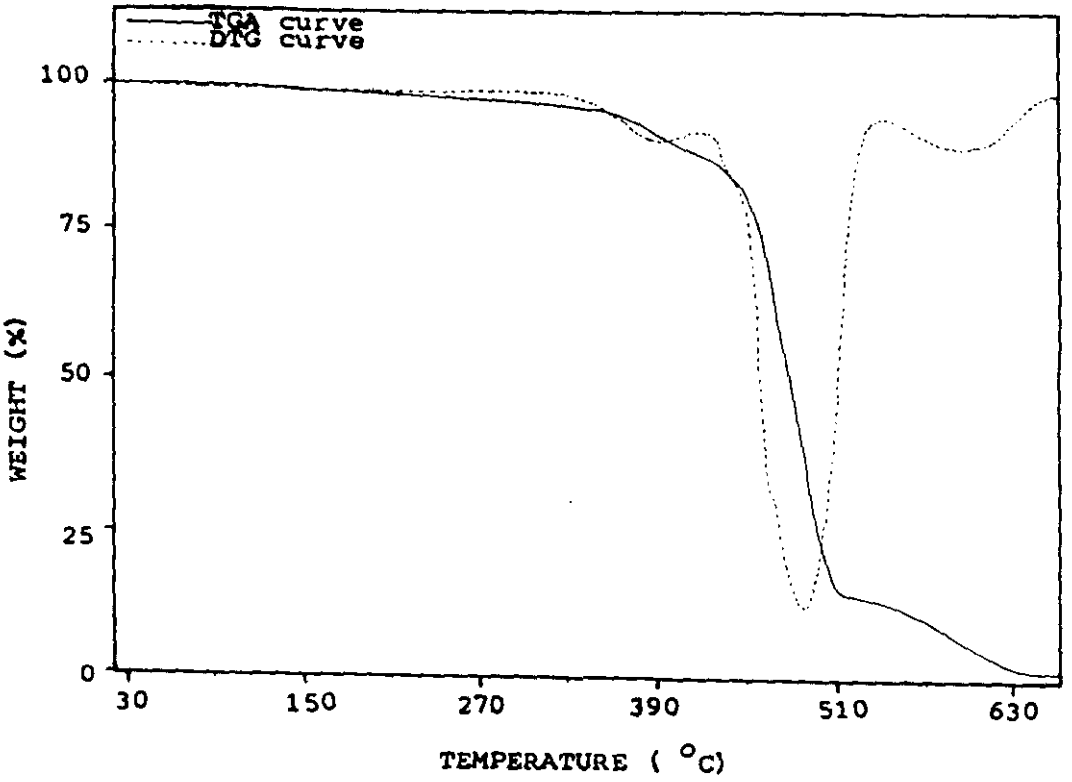

Figure 8.5. TG and DTG curves of $N_{70}P$

The blends $N_{30}P$ and $N_{50}P$ show two peaks in the DTG curve. The first peak around 390°C corresponds to the deacetylation from the vinyl acetate segments of EVA and the second peak around 490°C is a merged one of EVA and NBR In $N_{70}P$ three peaks are observed in the DTG curve. In this case the third peak at about 600°C corresponds to the degradation of acrylonitrile of NBR and this is observed only in the NBR rich blend. The initial and final decomposition temperatures of the blends are given in Table 8.1. It may be noted that as the NBR content increases, the initial and final decomposition temperatures are enhanced. The initial decomposition temperature (T_0) and the temperature of 50% decomposition (T_{50}) are plotted as a function of weight percentage of NBR in Figure 8.6. It is observed that both T_0 and T_{50} show a negative deviation from the additivity. However, an increase in the decomposition temperatures is observed with increase in NBR content. In Figure 8.7, the residue weight at different temperatures is plotted as a function of weight percentage of NBR. At 350°C, the residue weight of the pure components as well as the blends are nearly same. At 450 and 500°C, a slight increase in the residue weight is observed with the increase in the weight percent of NBR.

Table 8.1. Decomposition temperatures of different NBR/EVA blends

Samples	Initial decomposition temperature (°C)	Final decomposition temperature (°C)
N_0P	311	537
$N_{30}P$	341	544
$N_{50}P$	337	538
$N_{70}P$	342	655
$N_{100}P$	426	705
$N_{50}S$	321	541
$N_{50}M$	334	554
10S	334	544
10C	340	541
10BS	342	560
10BH	320	558
20BH	328	559
30BH	333	567

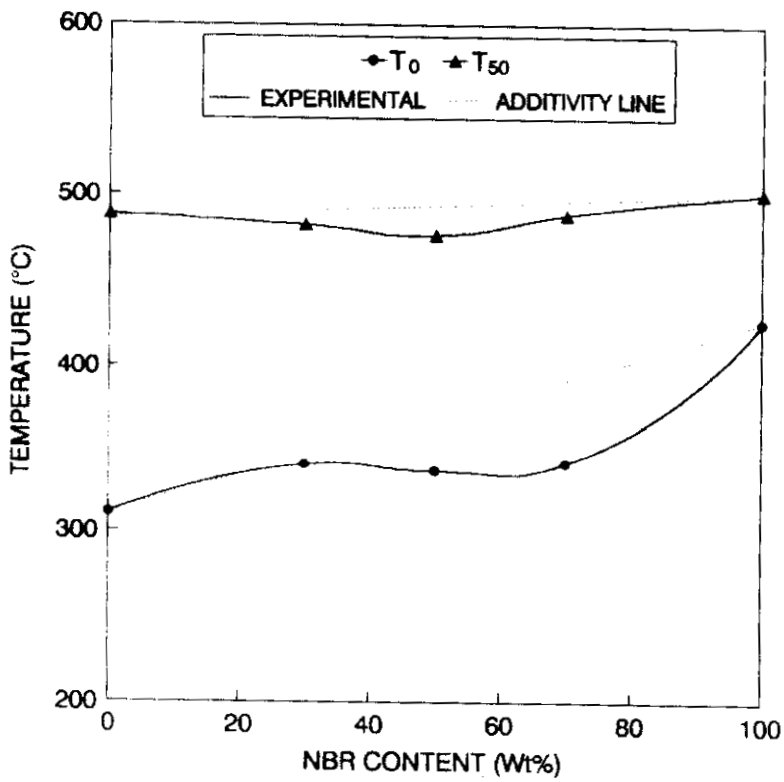

Figure 8.6. Variation in T_0 and T_{50} with weight % of NBR

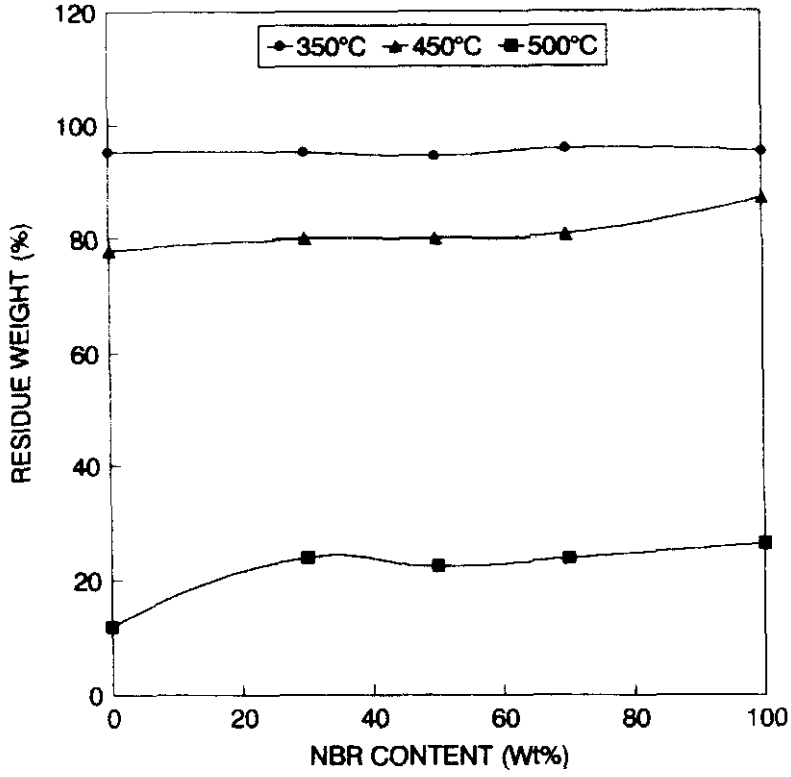

Figure 8.7. Variation in residue weight with weight % of NBR

(b) Effect of crosslinking systems

For the different crosslinking systems the initial decomposition temperature is 321, 337 and 334°C for the sulphur (S), peroxide (P) and mixed (M) cure systems respectively (Table 8.1). Here the peroxide cured system shows the highest initial decomposition temperature indicating a good thermal stability. This can be explained on the basis of the structure of networks (Figure 4.7) formed during vulcanisation and its respective bond lengths and bond energies (Table 8.2). The C-C linkages in the peroxide cured system is less flexible with the highest bond energy. The TG and DTG curves of $N_{50}S$ and $N_{50}M$ are given in Figures 8.8 and 8.9 respectively and $N_{50}P$ is shown in Figure 8.4. All the DTG curves show two peaks i.e., at (387, 504°C), (387, 493°C) and (386, 495°C) for sulphur,

peroxide and mixed cure systems respectively. The weight loss observed at 350 and 475°C is given in Table 8.3. Here also the peroxide cured system shows the lowest weight loss at a particular temperature.

Table 8.2. Bond length and bond energies of different types of chemical linkages

Type of bond	Bond length (Å)	Bond energy (kcal mol^{-1})
C-C	1.54	85
C-S	1.81	64
S-S	1.88	57

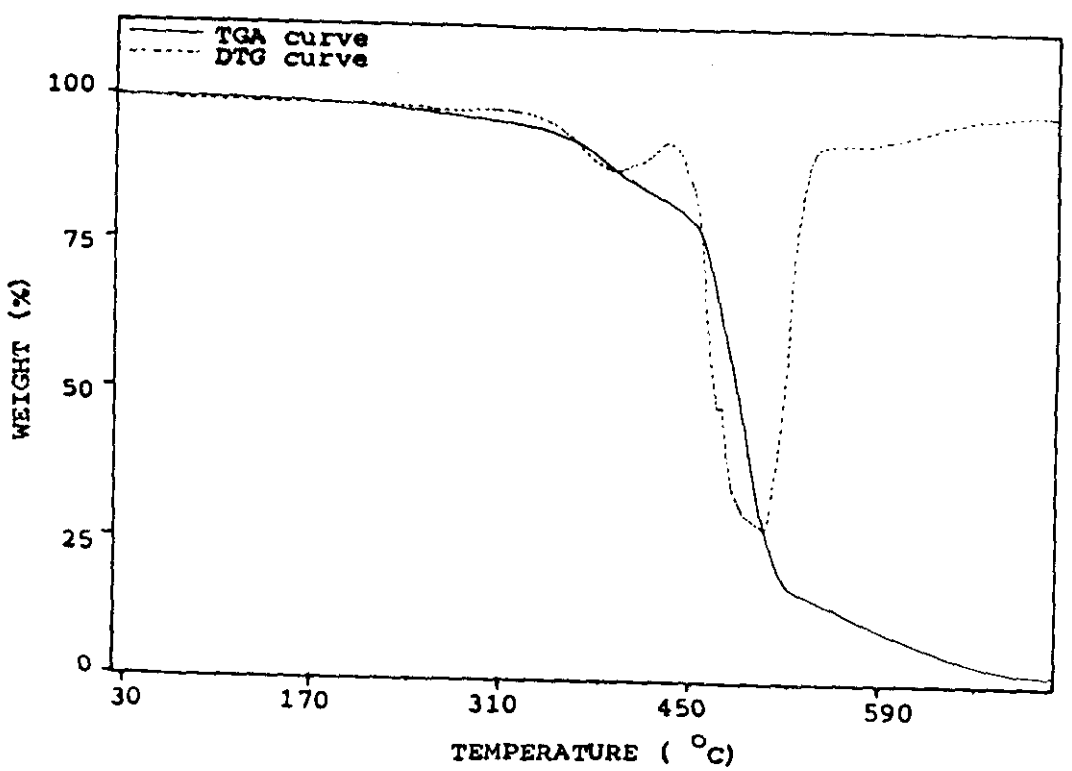

Figure 8.8. TG and DTG curves of $N_{50}S$

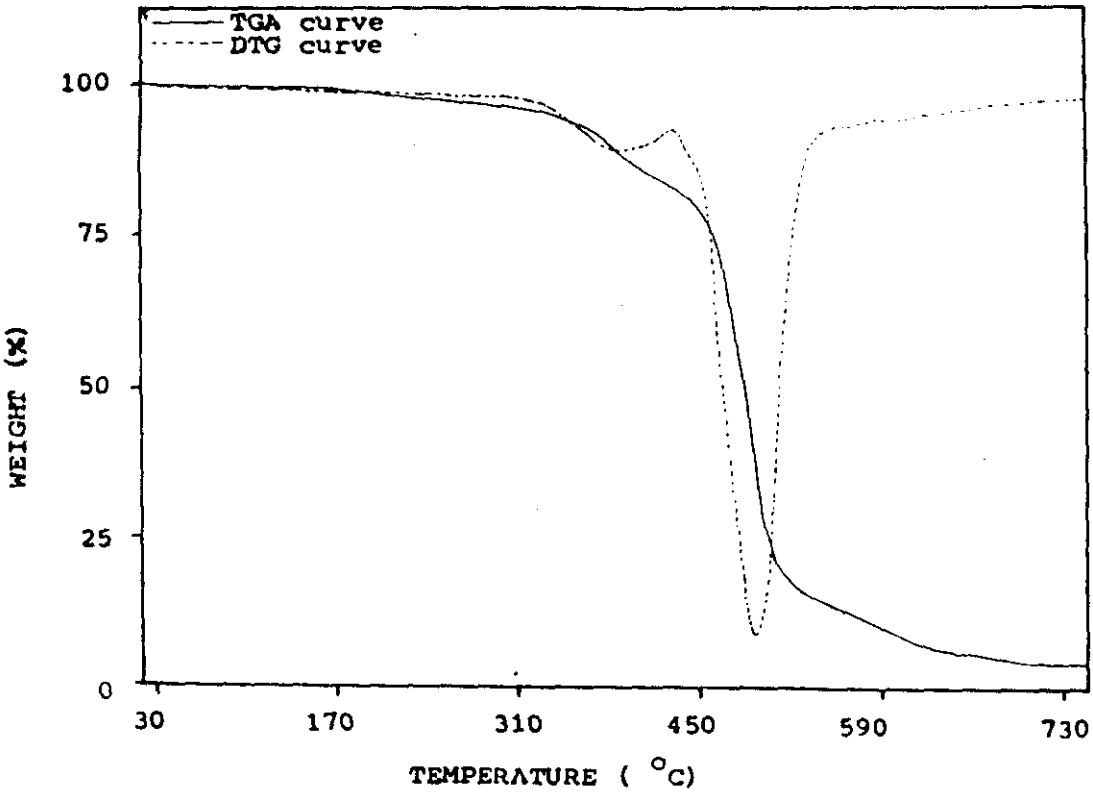

Figure 8.9. TG and DTG curves of $N_{50}M$

Table 8.3. Weight loss obtained from TGA of different NBR/EVA blends

Samples	Weight loss at 350°C (%)	Weight loss at 475°C (%)	Total weight loss (%)
N_0P	4.8	43.4	98.1
$N_{30}P$	4.8	33.7	93.8
$N_{50}P$	5.5	38.9	89.4
$N_{70}P$	4.1	42.0	98.2
$N_{100}P$	4.8	33.1	98.4
$N_{50}S$	6.2	42.7	96.1
$N_{50}M$	6.2	39.3	86.4
10S	5.5	33.1	91.3
10C	4.8	32.4	91.4
10BS	4.1	31.7	85.2
10BH	4.1	27.5	98.8
20BH	4.8	25.5	98.8
30BH	3.7	25.0	72.0

(c) Effect of fillers

In the case of the filled NBR/EVA ($N_{50}P$) system, the initial decomposition temperatures are marginally affected (Table 8.1). But there is an increase in the final decomposition temperature on addition of filler in all cases. With increase in filler loading (10BH, 20BH and 30BH) there is an improvement in the initial as well as final decomposition temperatures. The thermogravimetric and its derivative curves of the filled systems are given in Figures 8.10–8.15. All the DTG curves show two peaks—a minor one around 390°C and a major one around 500°C. From Table 8.1, it can be seen that the weight loss at 350 and 475°C is low for all the filled systems compared to the unfilled one ($N_{50}P$). This indicates the improvement in the thermal stability of the system with the addition of fillers.

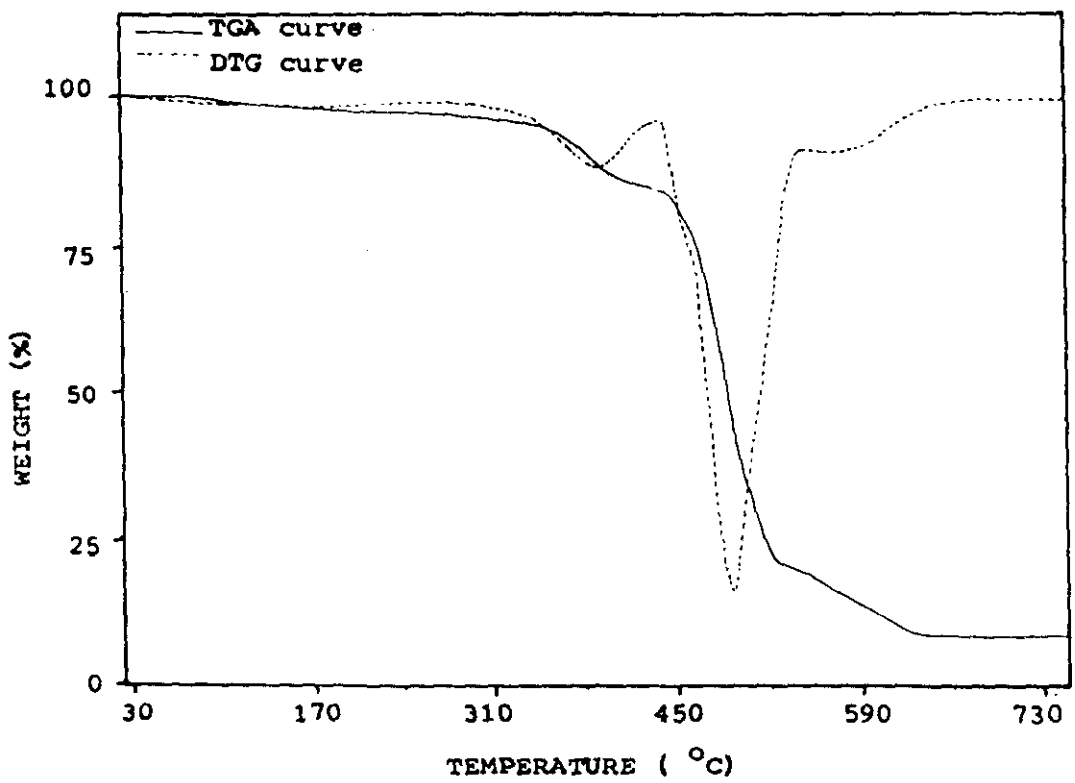

Figure 8.10. TG and DTG curves of 10 phr silica filled $N_{50}P$

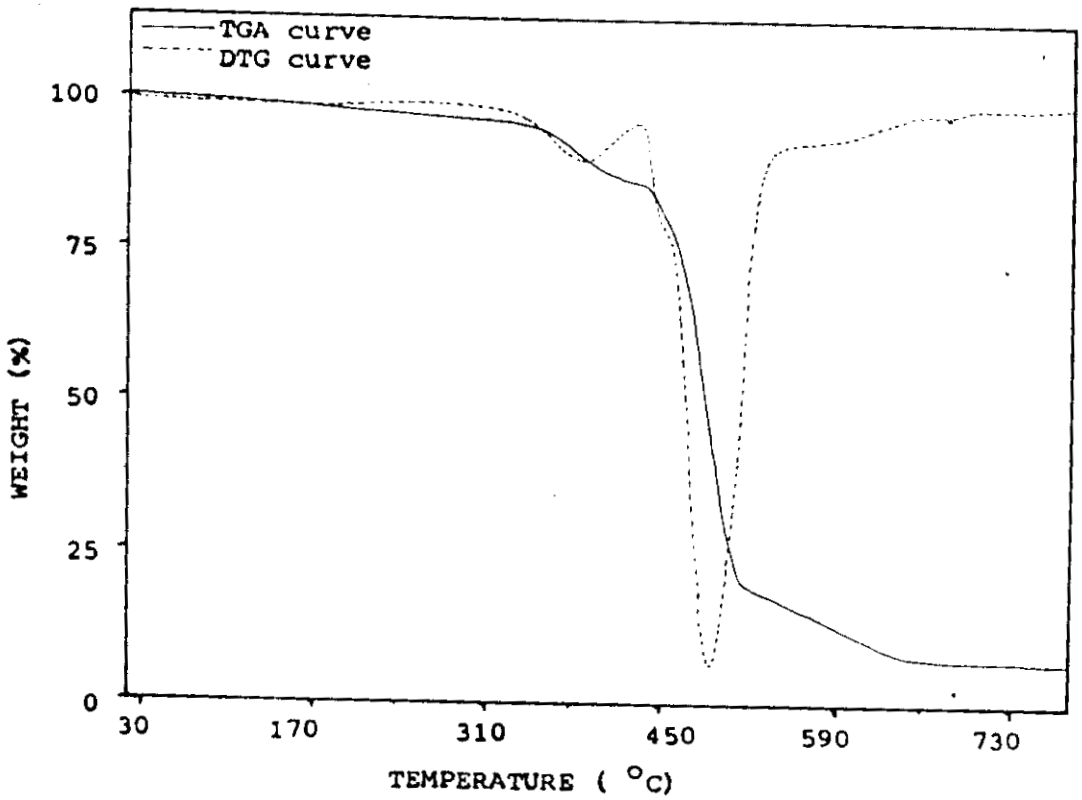

Figure 8.11. TG and DTG curves of 10 phr clay filled $N_{50}P$

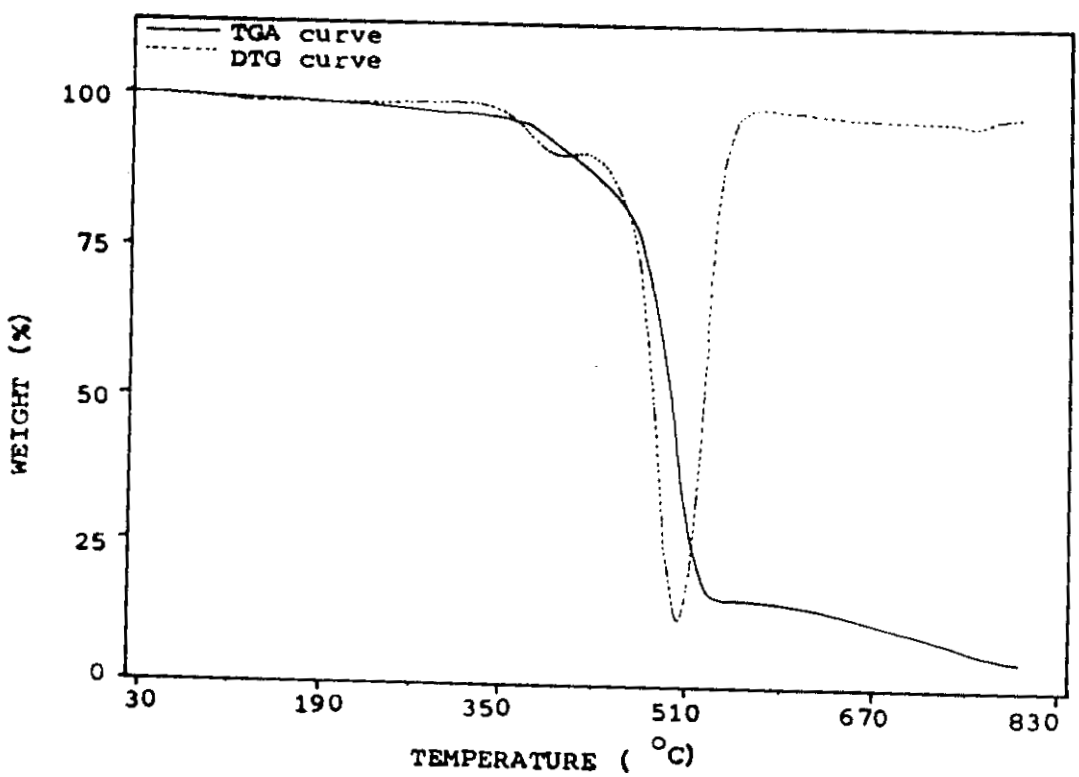

Figure 8.12. TG and DTG curves of 10 phr SRF filled $N_{50}P$

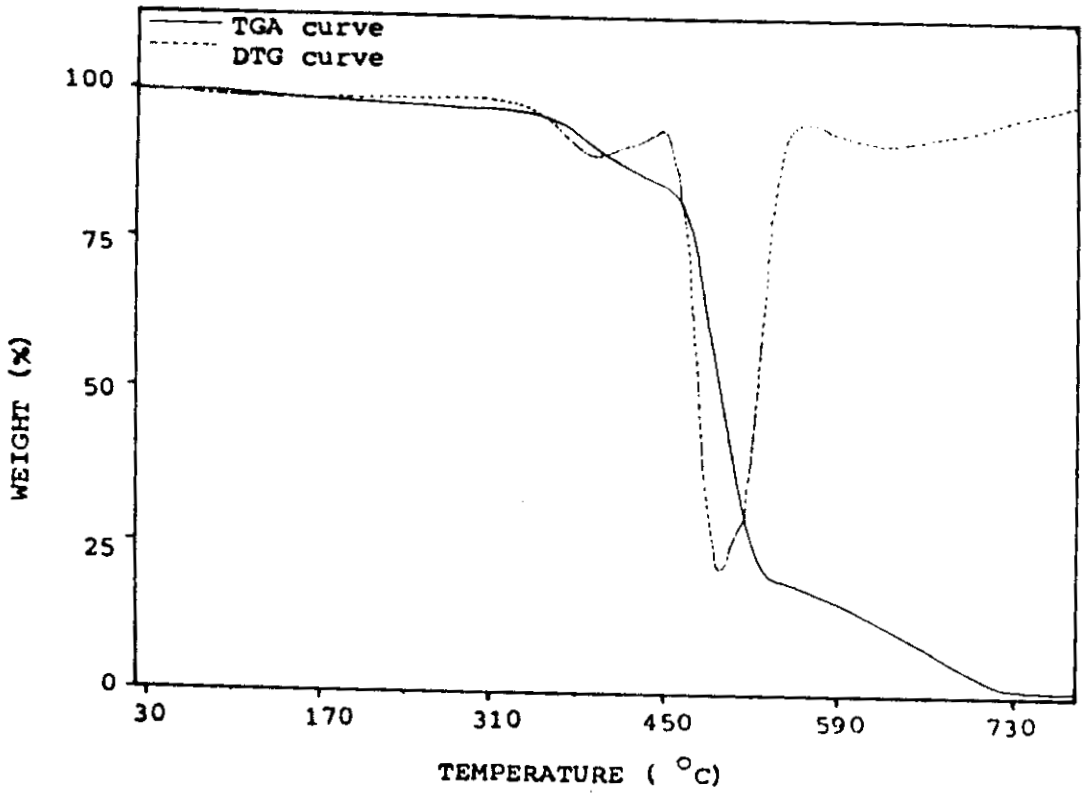

Figure 8.13. TG and DTG curves of 10 phr HAF filled $N_{50}P$

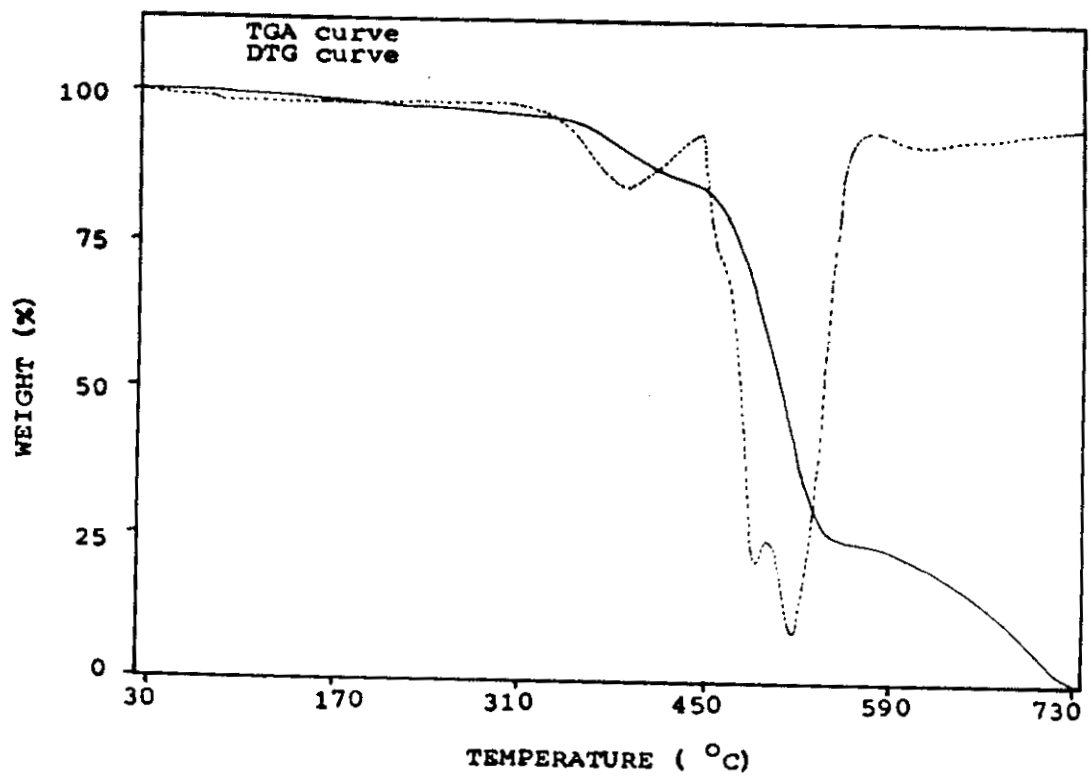

Figure 8.14. TG and DTG curves of 20 phr HAF filled $N_{50}P$

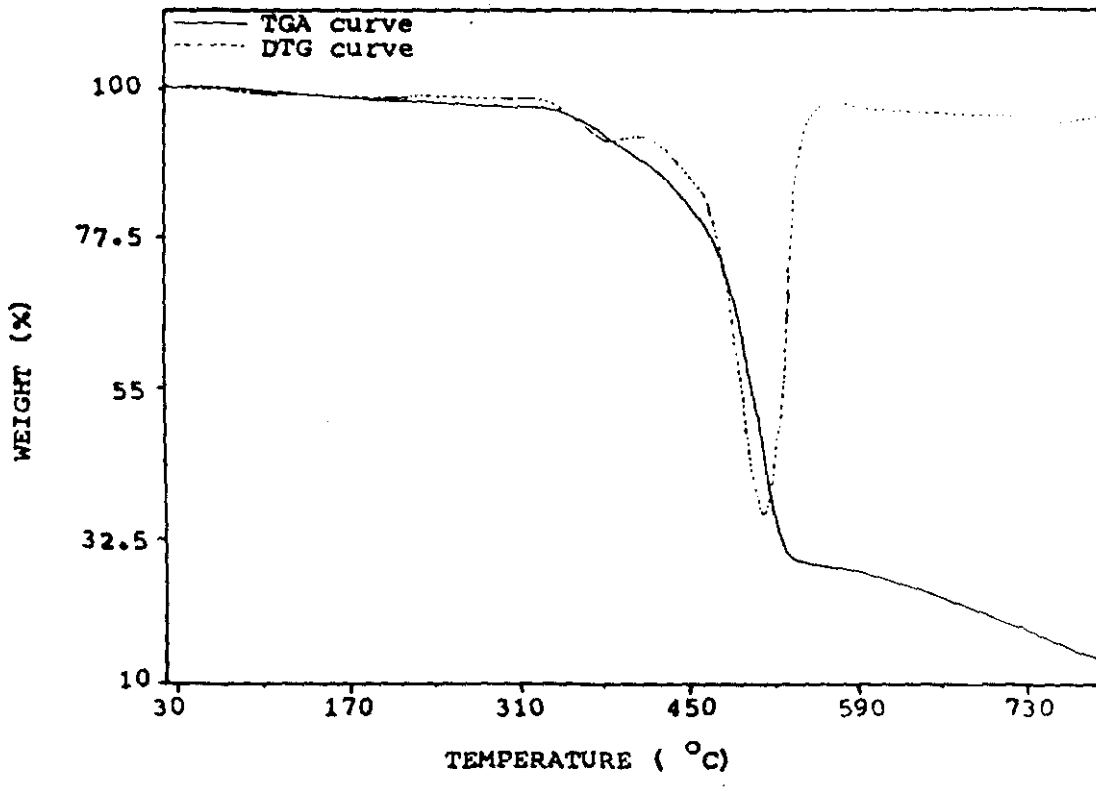

Figure 8.15. TG and DTG curves of 30 phr HAF filled $N_{50}P$

(d) Activation energy of degradation

The activation energy for the degradation process was calculated from the Arrhenius relationship given in Section 6.1.2. Here X is the weight loss at a particular temperature. The activation energy for degradation of the blends is plotted as a function of blend composition in Figure 8.16. It is seen that the blends exhibit a higher activation energy than the pure components indicating the thermal stability achieved by blending. The activation energy for the degradation process of all the systems is given in Table 8.4. Among the various crosslinking systems, the peroxide cured system shows the highest activation energy for the process. This is due to the nature of networks (Figure 4.7) and its respective bond lengths

and bond energies as explained earlier. In the mixed cure system, both types of linkages are present and its activation energy is close to that of the sulphur cured system. Among the various fillers used, the silica filled system shows the highest activation energy.

Table 8.4. Activation energy for degradation and property retention after ageing for NBR/EVA blends

Samples	Activation energy ($kJmol^{-1}$)	Retention in tensile strength after ageing at 100°C for 72 h (%)
N_0P	2.47	91
$N_{30}P$	3.01	92
$N_{50}P$	3.60	97
$N_{70}P$	4.21	94
$N_{100}P$	3.19	90
$N_{50}S$	2.94	80
$N_{50}M$	2.91	85
10S	3.20	81
10C	2.79	74
10BS	2.82	76
10BH	2.94	79
20BH	2.33	80
30BH	1.85	84

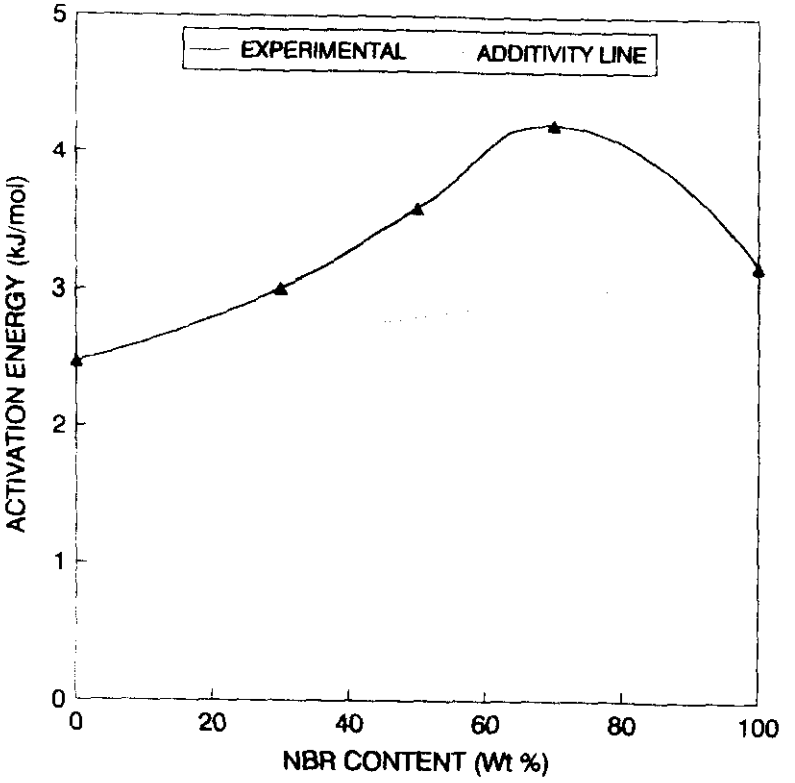

Figure 8.16. Effect of blend composition on the activation energy for degradation

8.1.2 Differential scanning calorimetry

The thermal behaviour of uncrosslinked and crosslinked NBR/EVA blends was analysed by DSC. The DSC traces of NBR, EVA and 50/50 NBR/EVA blend are shown in Figure 8.17. The mid point of the transition was recorded as the glass transition temperature (T_g). The T_gs of pure NBR and EVA are found to be -29.3 and -24.8°C and that of the 50/50 blend is -32.5°C. The downward peak around 80°C for N_0(EVA) and N_{50} is due to the melting of EVA. This peak is absent in the case of NBR. In the dynamic mechanical analysis also the peak due to the melting of EVA is observed around 80°C. The DSC traces of the uncrosslinked (N_{50}) and crosslinked systems ($N_{50}P$, $N_{50}S$ and $N_{50}M$) are compared in Figure 8.18. Introduction of crosslinks shifted the T_g towards a higher temperature. As observed in DMA, here also the mixed cure system ($N_{50}M$) with the highest crosslink density exhibits the highest T_g. The T_g and T_m (melting temperature) of uncrosslinked and crosslinked blends are given in Table 8.5.

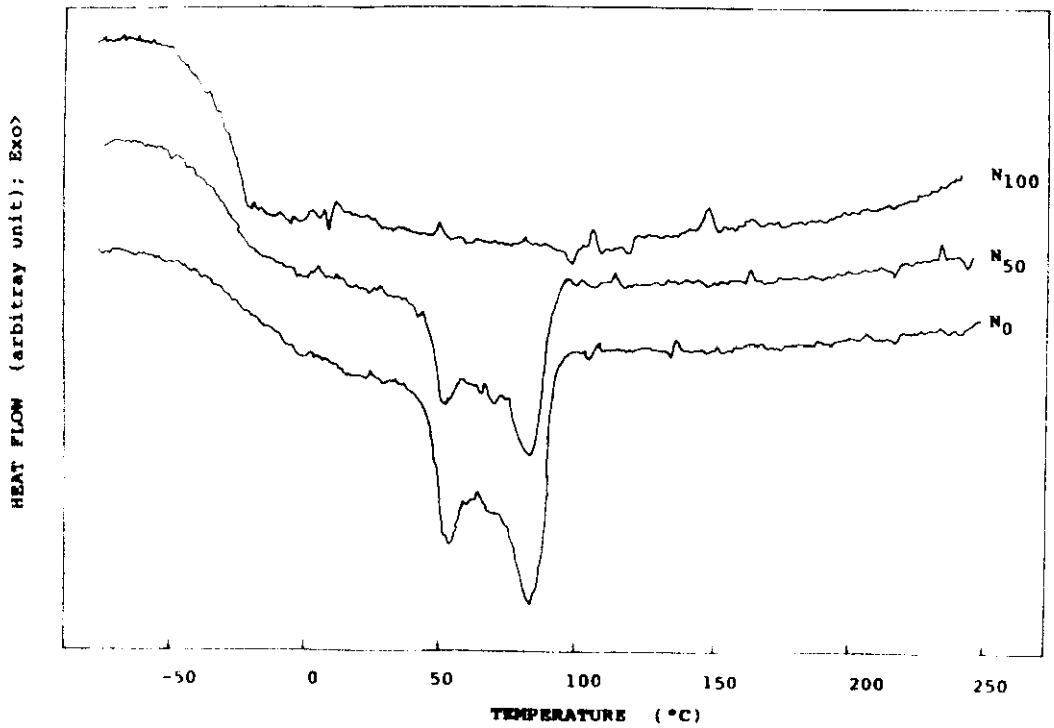

Figure 8.17. DSC curves of NBR/EVA blends

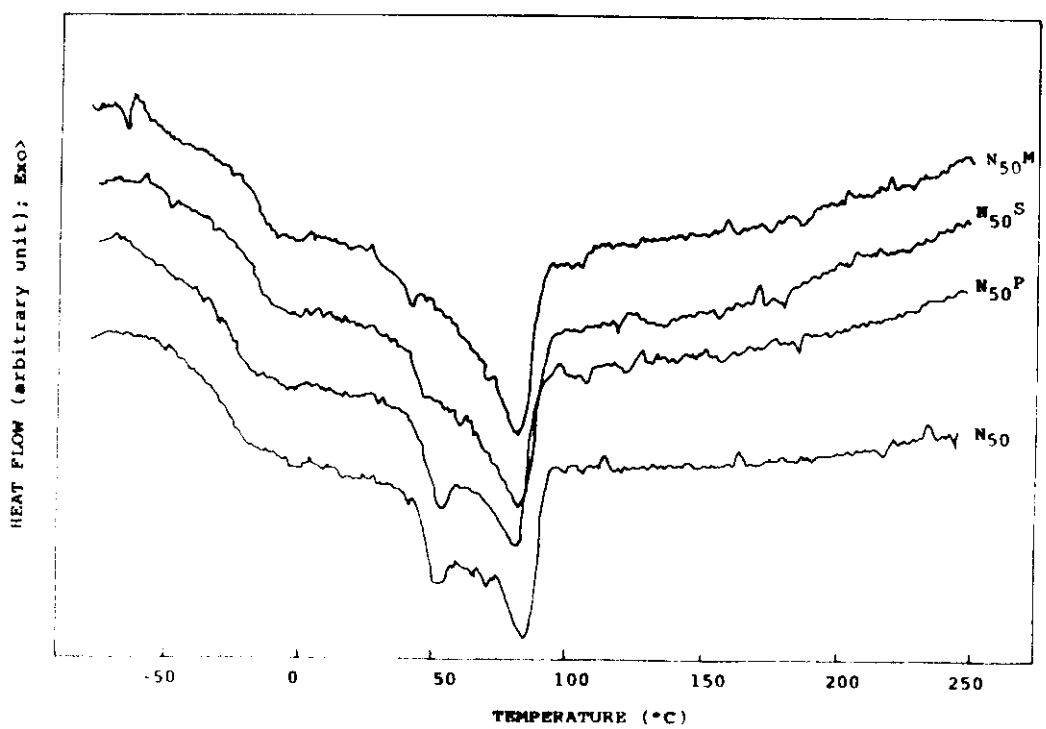

Figure 8.18. DSC curves of uncrosslinked and crosslinked $N_{50}P$

Table 8.5. T_g and T_m of NBR/EVA blends obtained calorimetrically

Sample code	T_g(°C)	T_m(°C)
N_0	-24.8	83.7
N_{50}	-32.5	83.8
N_{100}	-29.3	–
$N_{50}P$	-25	81.2
$N_{50}S$	-24	82.5
$N_{50}M$	-17	81.1

8.1.3 *Ageing characteristics*

(a) Thermal ageing

The results of thermal ageing of NBR/EVA blends as a function of blend composition, crosslinking systems, filler type (at 10 phr loading) and loading (HAF) are presented in Figures 8.19-8.22 respectively.

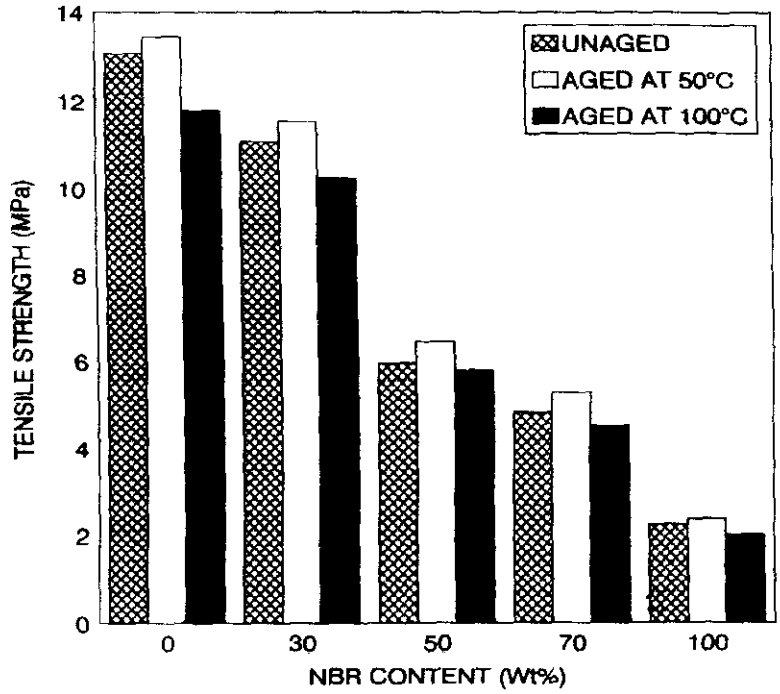

Figure 8.19. Effect of blend composition on the tensile strength of peroxide cured unaged and aged samples

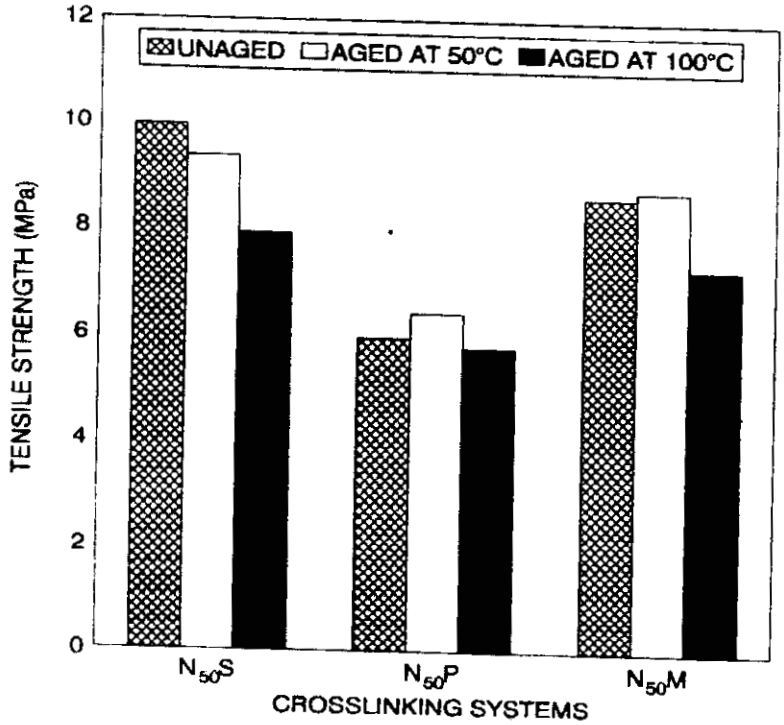

Figure 8.20. Effect of crosslinking systems on the tensile strength of unaged and aged samples

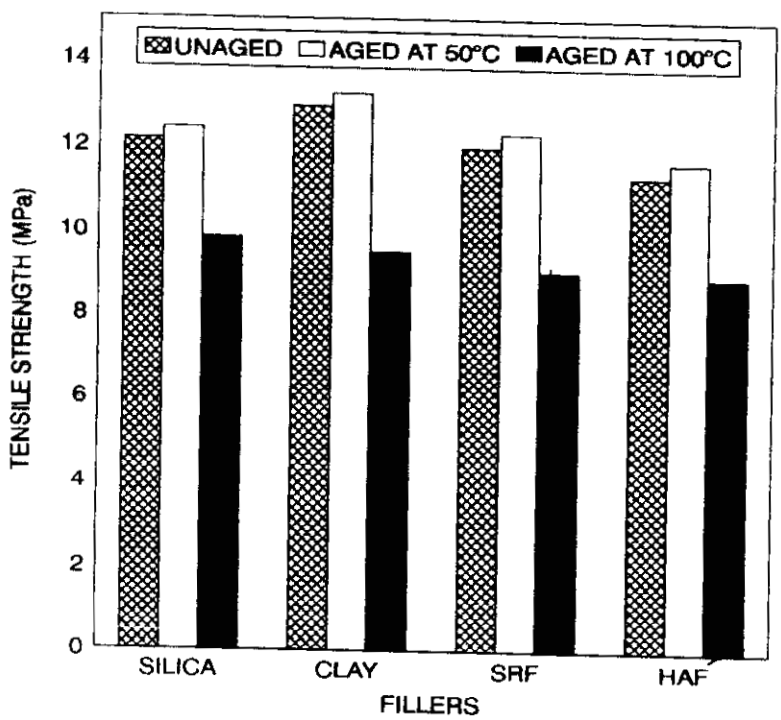

Figure 8.21. Effect of fillers on the tensile strength of unaged and aged samples

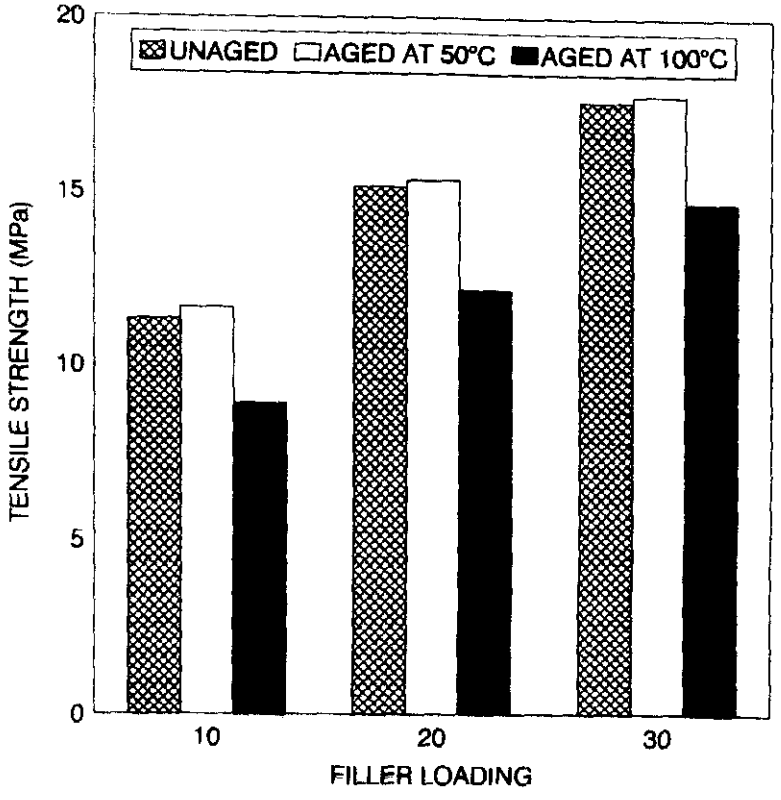

Figure 8.22. Effect of filler loading (HAF) on the tensile strength of unaged and aged samples

It is observed that the tensile strength of the blend system is nearly the same after ageing at 50°C for 72 h. This is further supported by the crosslink density values (Table 8.6) which are only marginally changed on ageing. The crosslink density is determined from the swelling method as explained in Section 2.3.7(b). It is important to notice that in all cases, the properties decrease after ageing at 100°C. This is due to the disintegration of crosslinks at an elevated temperature. The crosslink density also decreases after ageing at 100°C (Table 8.6).

Table 8.6. Crosslink density values of NBR/EVA blends

Samples	Crosslink density x 10^4 (gmol/cc)		
	Unaged	Aged at 50°C	Aged at 100°C
N_0P	16.88	16.97	16.69
$N_{30}P$	5.21	5.32	5.20
$N_{50}P$	2.84	3.02	2.84
$N_{70}P$	0.60	0.69	0.56
$N_{100}P$	0.95	1.07	0.89
$N_{50}S$	3.01	2.94	2.84
$N_{50}M$	3.25	3.37	3.02
10S	4.12	4.23	3.98
10C	4.02	4.19	3.94
10BS	4.28	4.33	4.25
10BH	4.55	4.62	4.42
20BH	5.01	5.09	4.97
30BH	5.07	5.14	5.03

After severe ageing condition at 100°C, the sulphur cured system retains only 80% of the property. For the peroxide and mixed cure systems, the retention in property was 97 and 85% respectively. This implies that, among the different crosslinking systems, peroxide cured system exhibits the best retention in property even after severe ageing condition. This is due to the thermal stability of the peroxide cured system as evident from the thermogravimetric studies discussed earlier. The retention in property after ageing of the blends is given in Table 8.4.

The stress-strain curves of aged and unaged samples of N_0P, $N_{50}P$ and $N_{100}P$ are given in Figures 8.23–8.25 The aged and unaged samples show similar stress-strain behaviour Due to the reduced strength the failure stress of the samples aged at 100°C occurs at a lower position in the stress-strain curve.

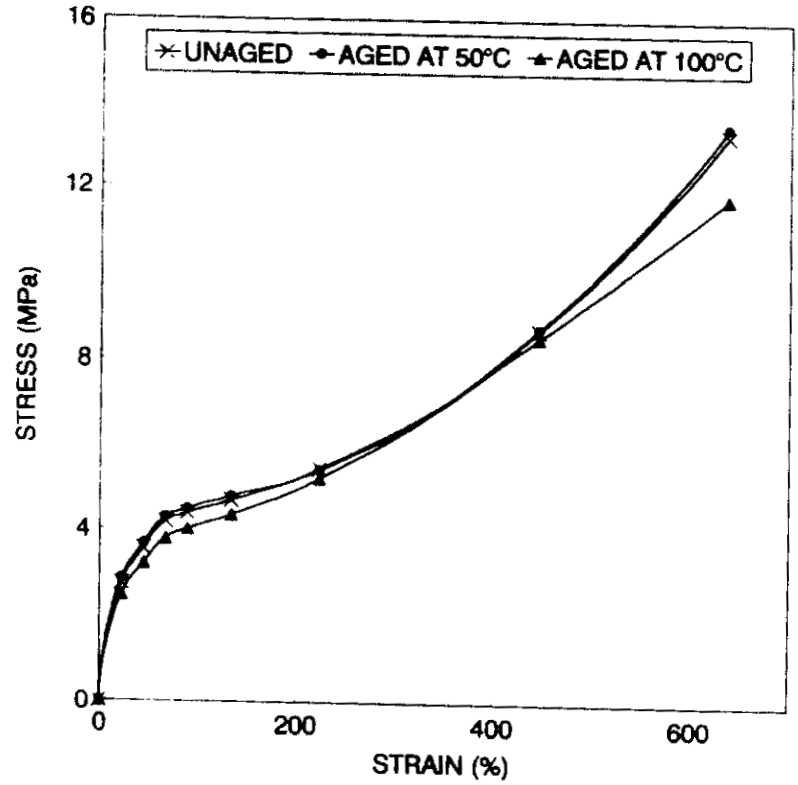

Figure 8.23. The stress-strain curves of unaged and aged N_0P

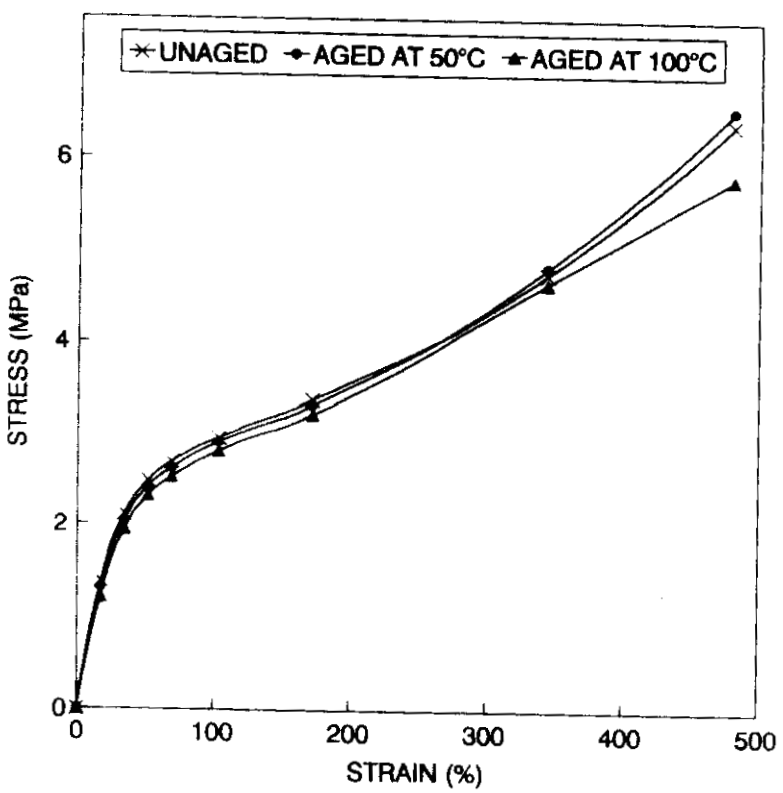

Figure 8.24. The stress-strain curves of unaged and aged $N_{50}P$

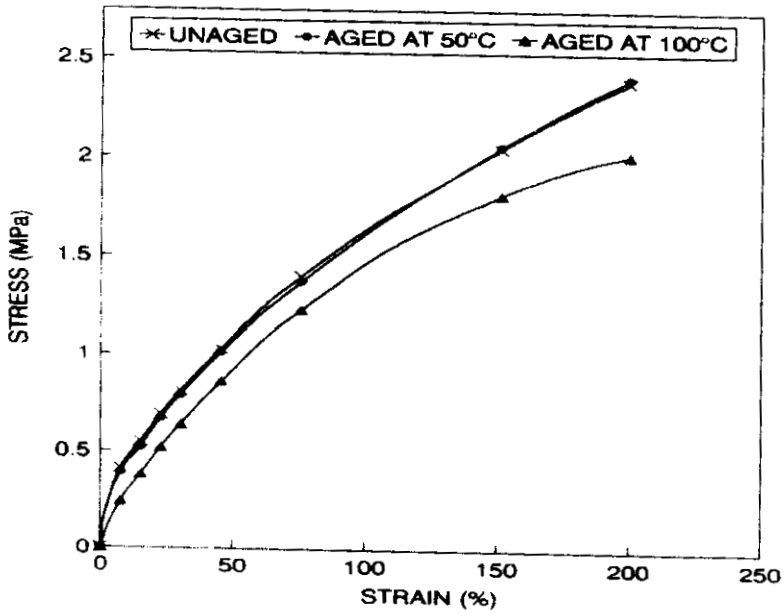

Figure 8.25. The stress-strain curves of unaged and aged $N_{100}P$

The tensile strength, elongation at break and young's modulus of the aged and unaged samples are plotted as a function of blend ratio in Figures 8.26-8.28. It is observed that the properties increase with increasing EVA content for both aged and unaged samples.

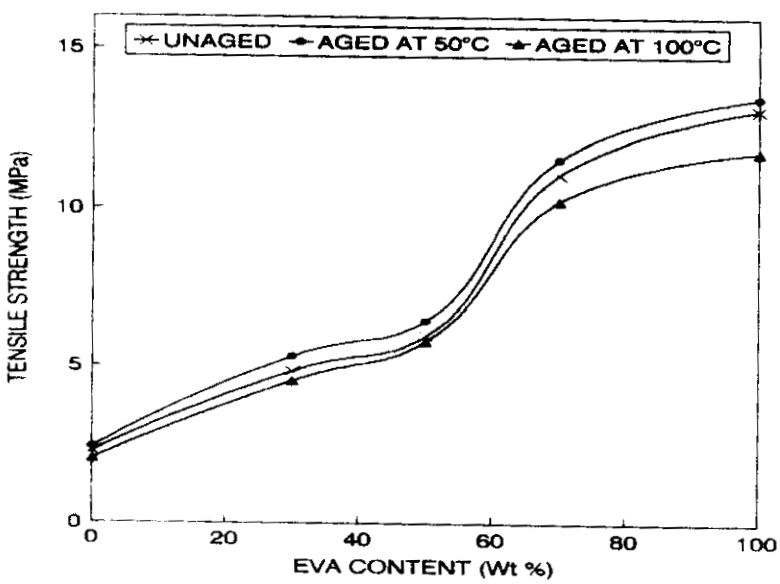

Figure 8.26. Dependence of tensile strength on the weight % of EVA for unaged and aged peroxide cured NBR/EVA blends

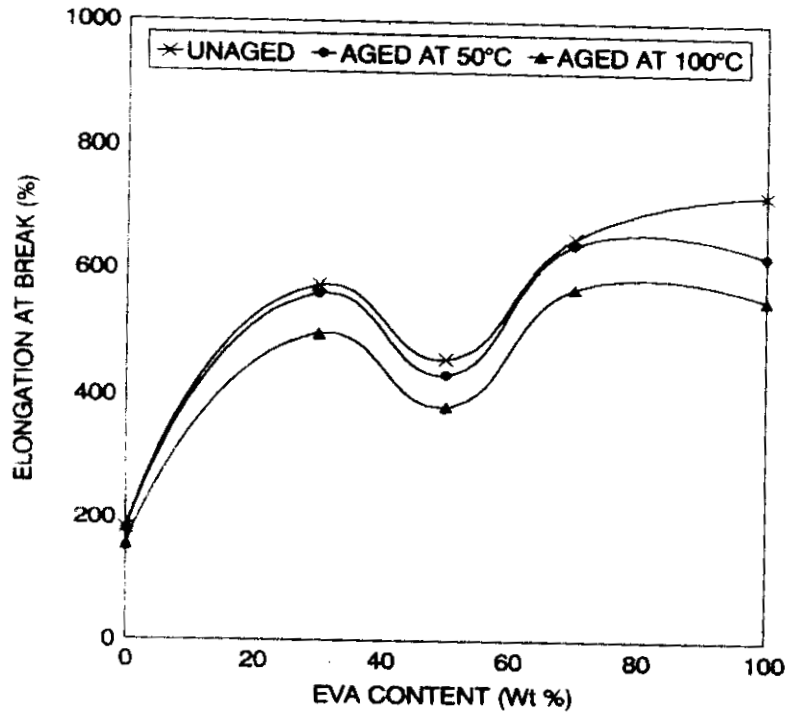

Figure 8.27. Variation in elongation at break, of unaged and aged peroxide and NBR/EVA blends, with the weight % of EVA

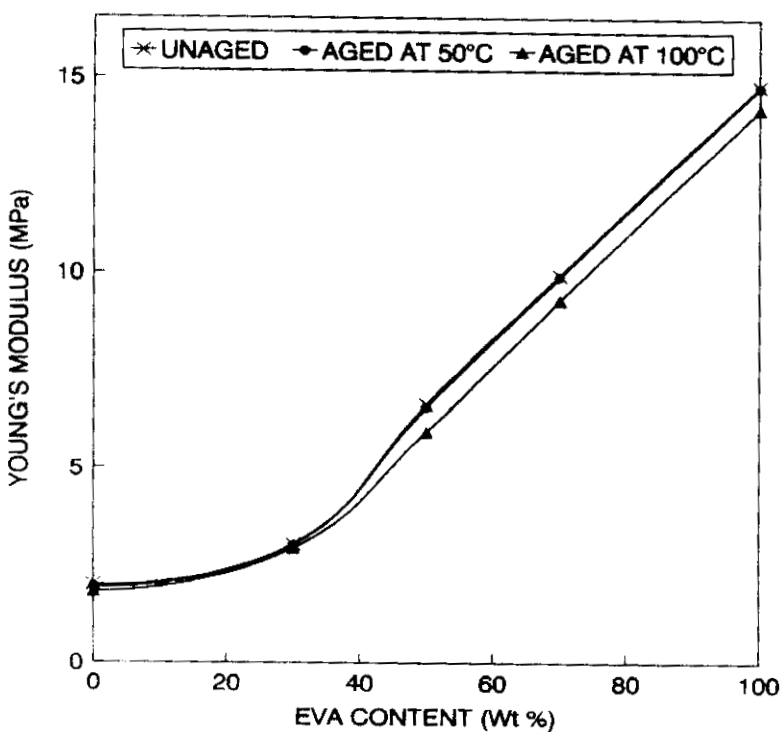

Figure 8.28. Variation in Young's modulus, of unaged and aged peroxide and NBR/EVA blends, with the weight % of EVA

It is also interesting to note that the properties are not adversely affected by the mild ageing condition (50°C for 72 h). But there is a decrease in properties for the samples aged at 100°C. This is due to the degradation of the crosslinks at a high temperature as explained earlier.

(b) Oil resistance studies

The oil resistance of the peroxide cured NBR/EVA blends is examined using aromatic, naphthenic and transformer oils. The percentage uptake is given in Table 8.7.

Table 8.7. Percentage uptake values for peroxide cured NBR/EVA blends

Samples	Percentage uptake		
	Aromatic oil	Naphthenic oil	Transformer oil
N_0P	9.8	13.3	12.7
$N_{30}P$	6.6	12.5	7.7
$N_{50}P$	4.9	10.8	5.3
$N_{70}P$	2.1	7.6	2.3
$N_{100}P$	1.6	6.5	1.5

As expected the percentage uptake decreases with NBR content. The blend exhibit better resistance to aromatic and transformer oils than to that of naphthenic oil. A considerable improvement in the oil resistance is observed with the addition of NBR.

8.2 References

1. I. C. McNeill, *Thermal Degradation*, in *Comprehensive Polymer Science-6*, (Ed., G. Allen), Pergamon Press, New York, 1989, Ch. 15.
2. E. A. Turi, *Thermal Characterisation of Polymeric Materials*, Vol. 1, Academic Press, New York, 1997.
3. K. T. Varughese, *Kauts. Gummi Kunst.*, **41**, 114 (1988).
4. K. T. Varughese, G. B. Nando, P. P. De and S. K. De, *J. Mater. Sci.*, **23**, 3894 (1988)
5. P. P. Lizymol and S. Thomas, *Polym. Deg. Stab.*, **41**, 59 (1993).
6. P. P. Lizymol and S. Thomas, *Thermochimica Acta*, **233**, 283 (1994).
7. L. Calandrelli, B. Immirzi, M. Malinconico, E. Martuscelli and F. Riva, *Makromol. Chem.*, **193**, 669 (1992).
8. I. A. Amraee, A. A. Katbab and SH. Aghafarajollah, *Rubber Chem., Technol.*, **69**, 130 (1995)
9. M. Patri, A. B. Samui and P. C. Deb, *J. Appl. Polym. Sci.*, **48**, 1709 (1993).
10. Carmen del Rio and J. L. Acosta, *Polym. International*, **30**, 47 (1993).
11. J. W. Cho, S. Tasaka and S. Miyata, *Polym. J.*, **25**, 1267 (1993).
12. A. T. Koshy, B. Kuriakose and S. Thomas, *Polym. Deg. Stab.*, **36**, 137 (1992).
13. S. Varghese, B. Kuriakose and S. Thomas, *Polym. Deg. Stab.*, **44**, 55 (1994).
14. K. Joseph, S. Thomas and C. Pavithran, *Comp. Sci. Technol.*, **53**, 99 (1995).
15. R. A. Emmett, *Ind. Eng. Chem.*, **36**, 730 (1944).
16. J. S. Noland, N. N. C. Hsu, R. Saxon and J. M. Schmitt, *Adv. Chem. Ser.*, **99**, 15 (1971).
17. P. J. Corish and B. D. W. Powell, *Rubber Chem. Technol.*, **47**, 481 (1974).
18. T. Skowronski, J. F. Rabek and B. Ranby, *Polym. Eng. Sci.*, **24**, 278 (1984).
19. J. R. Dunn, *Rubber Chem. Technol.*, **41**, 182 (1968).
20. S. D. Razumorskii and G. E. Zaikor, in *Developments of Polymer Stabilization-6*, (Ed., G. Scott), Applied Science Publishers, London, 1982.
21. Grassie, *Encycl. Polym. Sci. Technol.*, John Wiley and Sons. Inc., New York, Vol. 4, 1967. p. 159.